Intermolecular Cross-Linking of Na^+-Ca^{2+} Exchanger Proteins: Evidence for Dimer Formation†

Xiaoyan Ren, Debora A. Nicoll, Giselle Galang, and Kenneth D. Philipson*

Departments of Physiology and Medicine and the Cardiovascular Research Laboratories, David Geffen School of Medicine at UCLA, Los Angeles, California 90095-1760

Received January 30, 2008; Revised Manuscript Received April 1, 2008

ABSTRACT: The cardiac Na^+-Ca^{2+} exchanger (NCX1) is modeled to contain nine transmembrane segments (TMS) with a pair of oppositely oriented, conserved sequences called the α-repeats that are important in ion transport. Residue 122 in the α-1 repeat is in proximity to residue 768 in TMS 6, and the two residues can be cross-linked (*1*). During studies on the substrate specificity of this intramolecular cross-link, we found evidence that NCX1 can form dimers. At 37 °C in the absence of extracellular Na^+, copper phenanthroline catalyzes disulfide bond formation between cysteines at position 122 in adjacent NCX1 proteins. Dimerization was confirmed by histidine tag pull-down experiments that demonstrate the association of untagged NCX1 with histidine-tagged NCX1. Dimerization occurs along a face of the protein that includes parts of the α-1 and α-2 repeats as well as parts of TMS 1 and TMS 2. We do not see cross-linking between residues in TMS 5, TMS 6, or TMS 7. These data provide the first evidence for dimer formation by the Na^+-Ca^{2+} exchanger.

The Na^+-Ca^{2+} exchanger (NCX1[1]) is the primary cellular Ca^{2+} efflux mechanism of cardiomyocytes and plays an important role in the excitation−contraction−relaxation cycle. NCX1 transports one Ca^{2+} ion in exchange for three or four Na^+ ions (*2–4*). NCX1 can operate in both a Ca^{2+} efflux (or forward) and a Ca^{2+} influx (or reverse) mode. The net direction in which the exchanger will move Ca^{2+} is determined by the Na^+ and Ca^{2+} gradients and by the membrane potential. Under physiological conditions, NCX1 works primarily in the Ca^{2+} extrusion mode (*5*). However, when intracellular Na^+ is elevated, the amount of Ca^{2+} influx through NCX1 can increase substantially.

The current model for NCX1 (Figure 1) is composed of 9 transmembrane segments (TMSs) with a large intracellular loop between TMSs 5 and 6. The large intracellular loop has two Ca^{2+} regulatory domains (*6*). Functionally important repeat regions, α-1 and α-2, encompass TMSs 2 and 3 and TMS 7 and an intracellular segment, respectively. We have developed a helix-packing model that includes TMSs 1, 2, 3, 6, 7, and 8 (*1, 7*).

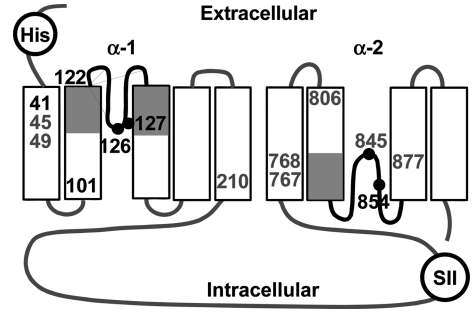

FIGURE 1: Topological model of the cardiac Na^+-Ca^{2+} exchanger. Transmembrane segments are indicated with rectangles, and the α-repeat regions are shaded. Numbers indicate amino acid residues that were mutated to cysteine in this study. Residues indicated by light font did not participate in dimer formation; residues in dark font could be cross-linked to form dimers. Sites of insertion of histidine (H) and StrepII (SII) tags are also shown.

The purified Na^+-Ca^{2+} exchanger displays three bands on SDS−PAGE with apparent molecular masses of 70, 120, and 160 kDa. The 70 kDa band is an active proteolytic fragment (*8*), and the 120 kDa band corresponds to the mature protein. Formation of an intramolecular disulfide bond between cysteine 792 and either cysteine 14 or 20 causes a mobility shift of the protein such that the mature protein migrates as a 140−160 kDa band (*9*).

NCX belongs to a superfamily of cation/Ca^{2+} exchange proteins (*10*) that includes $Na^+/Ca^{2+}-K^+$ exchangers, which exchange Na^+ for K^+ and Ca^{2+}. The $Na^+/Ca^{2+}-K^+$ exchanger has been shown to function as a monomer (*11*) but dimerizes (*12*) via apparent TMS interactions (*13*). To date, there is no evidence concerning the oligomeric state of the Na^+-Ca^{2+} exchanger. The aim of the present study was to assess the oligomeric state of NCX1 to further understand its operational mechanism. To this end, single-cysteine

† This work was supported by National Institutes of Health Grant HL-49101.

* Corresponding author. Department of Physiology, UCLA, 675 Charles E. Young Dr. S., MRL 3-645, Los Angeles, CA 90095-1760. Tel: 310-825-7679. Fax: 310-206-5777. E-mail: KPhilipson@mednet.ucla.edu.

[1] Abbreviations: NCX1, Na^+-Ca^{2+} exchanger; TMS, transmembrane segment; PAGE, polyacrylamide gel electrophoresis; MTS, methanethiosulfonate; MOPS, 4-morpholinepropanesulfonic acid; CuPhe, $CuSO_4$/phenanthroline; MTSES, sodium (2-sulfonatoethyl) methanethiosulfonate; MTSEA, 2-aminoethyl methanethiosulfonate hydrobromide; MTSET, [2-(trimethylammonium)ethyl]methanethiosulfonatebromide; NEM, *N*-ethylmaleimide. BMDB, 1,4-bismaleimidy-2,3-dihydroxybutane; $BM[PEO]_2$, 1,8-bismaleimidodiethylene glycol; TCEP, tris(2-carboxyethyl)phosphine; DTT, dithiothreitol; DDM, *n*-dodecyl-β-D-maltoside.

10.1021/bi800177t CCC: $40.75
Published on Web 05/09/2008

exchangers were heterologously expressed in *Drosophila* High Five cells. Subsequently, chemical cross-linking and pull-down experiments established a dimeric state of NCX1.

MATERIALS AND METHODS

Construction and Expression of NCX1 Mutants in Insect High Five Cells. Site-directed mutagenesis was performed as recently described (*1*). Some NCX1 mutants were modified to contain internal tags: an 8 histidine tag near the NH_2-terminus at amino acid N9 that removes the glycosylation site and a StrepII (WSHPQFEK) epitope tag in the large cytoplasmic loop after amino acid S655 (Figure 1). The StrepII site is within the flexible FG loop of a binding domain for regulatory Ca^{2+} (*6*). Exchangers containing both tags are denoted with the label 2-Tag and those with only the StrepII tag with the label S-Tag. High Five cells (Invitrogen) were transfected with mutant exchangers, and Na^+-Ca^{2+} exchange activity was measured as Na^+-gradient dependent $^{45}Ca^{2+}$ uptake into intact cells as described (*1*).

Cross-Linking Procedures. Cross-linking reactions with copper phenanthroline (CuPhe) were carried out as previously described (*1*) using Na^+ (10 mM Tris-HCl at pH 7.2, 150 mM NaCl) or Cs^+ (10 mM Tris-HCl at pH 7.2, 150 mM CsCl) cross-linking buffer. CuPhe was prepared as 1 mM $CuSO_4$ and 3 mM phenanthroline and is indicated as 1 mM CuPhe in the text. Alternatively, we used the cross-linkers 1,4-bismaleimidyl-2,3-dihydroxybutane (BMDB, Pierce) or 1,8-bismaleimidodiethylene glycol ($BM[PEO]_2$, Pierce) at 0.5 mM. In this case, intact cells were washed with Na^+ cross-linking buffer containing 5 mM EDTA, then cross-linking was carried out at 27 °C in the intact cell suspension and the reaction terminated after 30 min by addition of 10 mM DTT. The High Five cells are grown at 27−28 °C, but incubation at 22 or 37 °C for 20 min during cross-linking resulted in no observable change in cell morphology. After cross-linking, cells were dissolved with lysis buffer [1% Triton X-100 with Complete, EDTA-free Protease Inhibitors (Roche Applied Science)]. Aliquots of cell lysates were subjected to 7.5% SDS−PAGE in the absence of reducing reagents. Immunoblot analysis was carried out with NCX1 antibody R3F1 or C2C12 (*14*). Specific bands on immunoblots were quantitated as the fraction of total antibody-reacting protein using ImageJ software (*15*).

His Tag Pull Down. Cysteine mutants C122 and 2-Tag-C122 or cysteine-less and 2-Tag-cysteine-less were coexpressed in High Five cells on a 100 mm plate. Twenty-four hours after transfection, cross-linking was carried out in the Cs^+ buffer by the addition of 1 mM CuPhe at 37 °C for 10 min. The reaction was stopped by adding 5 mM MTSEA at room temperature for 10 min. Cells were solubilized with 40 mM *n*-dodecyl-β-D-maltoside (DDM) in washing buffer (100 mM Tris-HCl at pH 8, 300 mM NaCl). The supernatant was then incubated with Ni Sepharose 6 fast flow (GE Healthcare, Piscataway NJ) at 4 °C for 1 h with rotation. The beads were washed 3 times with washing buffer containing 10 mM DDM and 25, 30, and then 35 mM imidazole. Protein was eluted after a 5 min of incubation in washing buffer containing 250 mM imidazole. The elutate was diluted with 5× nonreducing sample buffer. Samples were run on nonreducing 7.5% SDS−PAGE and transferred to nitrocellulose. Immunoblot analysis was performed using NCX1 antibodies R3F1 or C2C12.

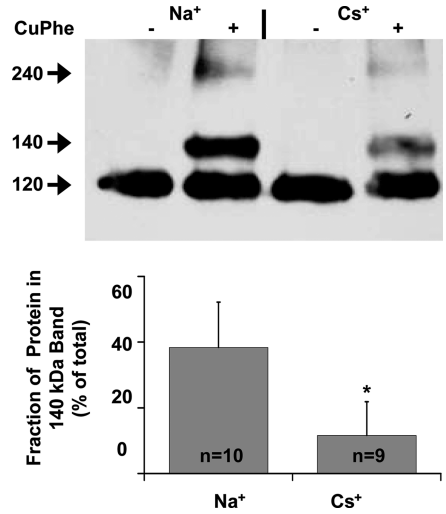

FIGURE 2: Intramolecular cross-linking between C122 and C768 is optimal in the presence of Na^+. Upper panel: Western blot showing intramolecular cross-linking induced by CuPhe (1 mM) as indicated by the band at 140 kDa band. Cross-linking reactions were performed in buffers containing either Na^+ or Cs^+ for 20 min at 22 °C. Lower panel: The percentage of total NCX1 protein forming an intramolecular cross-link (140 kDa) in the presence of CuPhe determined by densitometry. $*p < 0.01$ compared to Na^+ cross-linking condition.

RESULTS

Topological Model of NCX1. Figure 1 shows the positions of residues mutated to cysteine in this study. The cysteine-less exchanger, which has had all 15 endogenous cysteines mutated to alanine or serine (*16*), was used as the background for the introduction of cysteines. For some mutants, we reintroduced endogenous cysteines at positions122, 210, or 768, and for others, we introduced cysteines at new locations. Mutant exchangers are designated by the residues that have been changed to cysteine. For example, exchanger C122/C768 contains cysteines at position 122 and 768 in the cysteine-less background. For pull-down experiments, a His tag comprising 8 histidines was inserted near the NH_2-terminus at position 9, and a StrepII tag was inserted in the large intracellular loop at position 655 as shown in Figure 1. Exchangers with dual labels are referred to as 2-Tag exchangers.

Ion-Dependent Cross-Linking of NCX1 Mutant C122/C768. In previous work (*1*), we demonstrated that an intramolecular disulfide bond between either C14 or C20 in the NH_2-terminal half with C792 in the CO_2-terminal half of the exchanger results in a mobility shift from 120 kDa to 140−160 kDa (*1, 7, 9*) on SDS−PAGE. Using this approach, we showed that C122 and C768 are sufficiently close in the folded protein to form an intramolecular disulfide bond in the presence of CuPhe (*1*). C122 is located in the functionally important α-1 repeat region that may undergo conformational changes during the reaction cycle.

To investigate whether extracellular substrates affect the distance between residues C122 and C768, we examined cross-linking in the presence or absence of Na^+ at 22 (Figure 2) and 37 °C (Figure 3). We found that intramolecular cross-linking, as indicated by the appearance of a 140 kDa band,

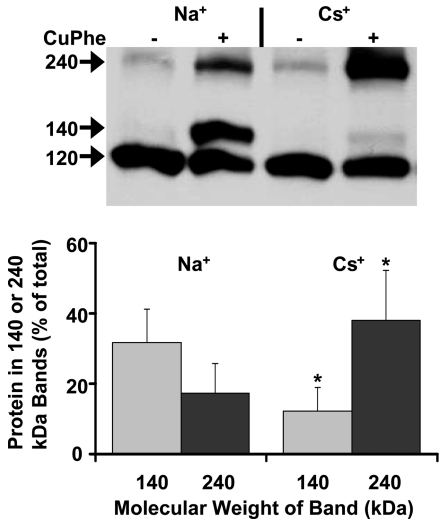

FIGURE 3: NCX1 dimer formation is enhanced at 37 °C in the absence of Na^+ for mutant C122/C768. Upper panel: Western blot showing intra- (140 kDa) or intermolecular (240 kDa) cross-linking in the presence of Na^+ or Cs^+. Cross-linking was catalyzed by CuPhe (1 mM) for 20 min at 37 °C. Lower panel: Percentage of total NCX1 protein forming intramolecular (140 kDa) or intermolecular cross-links (240 kDa). *$p < 0.01$ compared to Na^+ cross-linking conditions. $n = 8$.

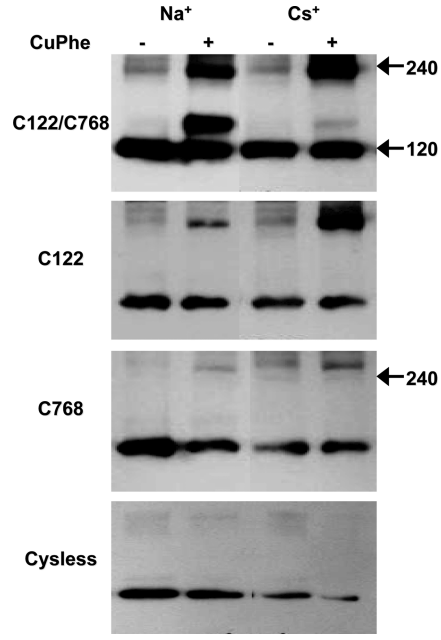

FIGURE 4: Residue C122 is responsible for CuPhe-catalyzed dimer formation in mutant C122/C768. Cross-linking reactions for the double cysteine (C122/C768), single cysteine (C122 and C768), or cysteine-less mutant were performed at 37 °C as described in Figure 3. The 240 kDa dimer band was only observed for the C122/C768 and the C122 mutants. Note that the weak upper molecular weight band seen with C768 is larger than 240 kDa. Data are representative of 3 or 4 experiments.

is optimal in the presence of extracellular Na^+ at 22 °C (Figure 2, upper panel). By densitometry, there is significantly less cross-linking in the absence of Na^+ (Figure 2, lower panel).

At 37 °C, an additional band at 240 kDa became prominent (Figure 3). Since this is twice the size of the monomeric 120 kDa band, we hypothesized that the 240 kDa band represents dimeric NCX1. In the absence of Na^+, the 240 kDa band is pronounced, and the 140 kDa band is greatly reduced. Thus, at 37 °C, intramolecular cross-linking is favored by the presence of Na^+, while dimer formation (intermolecular cross-linking) is favored by the absence of Na^+. Addition of Ca^{2+} (2 mM) to the Na^+ medium did not affect dimer formation but did decrease the amount of intramolecular cross-linking (not shown).

To confirm that cross-linked bands of mutant C122/C768 originated from cysteines within NCX1, we pretreated intact cells expressing the mutant NCX1 with the membrane impermeable reagents MTSET and MTSES or the membrane permeable reagents MTSEA and NEM prior to initiation of cross-linking procedures. The goal was to block accessible cysteines and thus prevent formation of CuPhe-induced disulfide bonds. Formation of both the 140 and 240 kDa bands was completely eliminated by preincubation with MTSEA (10 mM). MTSES (20 mM) reduced the intensity of the bands, while MTSET and NEM had little effect (data not shown). Apparently, C122 and C768 are accessible to MTSEA and MTSES but not to all sulfhydryl reagents.

Dimerization of NCX1 Is Mediated by C122. There are at least three possibilities to explain the appearance of an apparent dimer at 240 kDa upon expression of C122/C768. First, there may be cross-linking between the same residues of adjacent proteins, i.e., between two cysteines 122 or between two cysteines 768 of two NCX1 proteins. Second, cysteine 122 on one NCX1 may cross-link with cysteine 768 of another NCX1 protein. Finally, the 240 kDa band may be the result of NCX1 cross-linking with another protein that fortuitously results in a band with the molecular weight of the predicted dimer. To examine these possibilities, High Five cells were transfected with the mutants C122/C768, C122, C768, or cysteine-less NCX1. Cross-linking was performed at 37 °C for 20 min with 1 mM CuPhe. As shown in Figure 4, the 240 kDa band appeared only when a cysteine was present at position 122. Again, apparent dimer formation was more prominent in the Na^+-free medium. The data show that the cysteine at position 122 at the external end of TMS 2 can mediate dimer formation. Note that the 140 kDa band, due to an intramolecular disulfide bond, is completely absent in the single-cysteine mutants C122 and C768. This result further indicates that the 140 kDa band is due to an intramolecular linkage between C122 and C768.

In the panel (Figure 4) displaying data from mutant C768 as well as in Figures 5 and 6, we detected bands greater than 240 kDa. These higher molecular weight bands were observed in both CuPhe-treated and -untreated samples. The intensity and size of these bands were variable. The more prominent 240 kDa band was only present for certain mutants after CuPhe treatment as a specific indication of dimer formation. The origin of the higher molecular weight bands is uncertain but may be due to noncovalently bound higher order oligomers or nonspecific aggregation.

To confirm dimer formation, we performed pull-down experiments. We inserted two tags into NCX1 mutants. An 8-histidine tag was inserted into the glycosylation site at position 9. This tag was used to pull-down NCX1 using a Ni-affinity column. A second tag, StrepII, was in the large intracellular loop at position 655 (Figure 1). The StrepII tag disrupts the epitope for monoclonal antibody R3F1 (the epitope for R3F1 is between amino acids 560−705) but leaves the epitope for antibody C2C12 (amino acids 371−525)

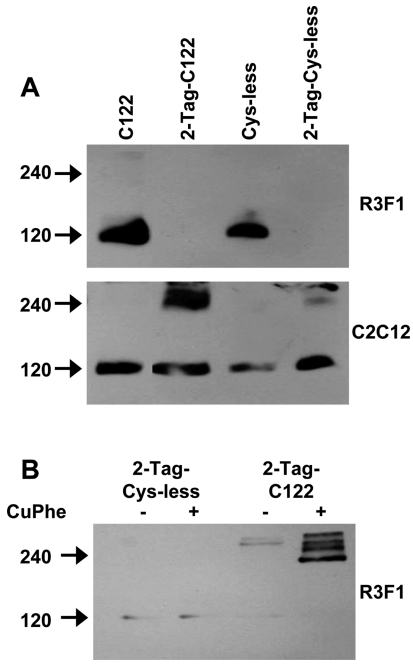

FIGURE 5: Pull-down experiments confirm that exchanger mutant C122 can form dimers. (A) Demonstration that tagged NCX1 proteins can be detected only with antibody C2C12 and not R3F1. Lysates from High Five cells expressing each of the mutants were probed with antibody R3F1 (top panel) or C2C12 (bottom panel). (B) His-tag pull-down products after cotransfection of NCX1 mutants. High Five cells coexpressing cysteine-less and 2-Tag-cysteine-less (lanes 1 and 2) or C122 and 2-Tag-C122 (lanes 3 and 4) were treated with CuPhe, then solubilized and bound to Ni-sepharose resin as described in Materials and Methods. Imidazole-eluted protein was detected with NCX1 antibody R3F1. Data are representative of nine experiments.

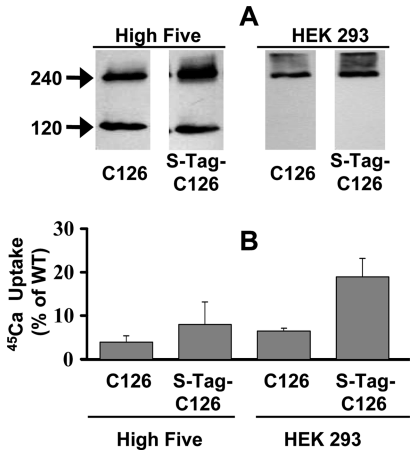

FIGURE 6: Dimerization detected in the single cysteine NCX1 mutant C126. (A) No catalyst is required for dimer formation with the C126 mutant. Cells were transfected with mutants C126 or S-Tag-C126 in High Five (left panel) or HEK 293 (right panel) cells, respectively. No CuPhe treatment was used. SDS−PAGE analysis was performed under nonreducing conditions in Na^+ cross-linking buffer as described in Materials and Methods. Protein was detected with NCX1 antibody C2C12. (B) Na^+ gradient-dependent $^{45}Ca^{2+}$ uptake in High Five (left) and HEK 293 (right) cells expressing C126 or S-Tag-C126 mutants. Data are presented as percentage of wild-type NCX1 activity.

intact (*14*). This is demonstrated in Figure 5A where lysates of High Five cells expressing mutant NCX1 proteins were examined by immunoblots probed with R3F1 (upper panel) or C2C12 (lower panel). No NCX1 protein was detected in cells expressing the 2-Tag NCX1s (lanes 2 and 4) with the R3F1 antibody. However, when the blot was probed with C2C12, NCX could be detected for all mutants. All 2-Tag NCX1 proteins are functional with levels of activity ranging from 20−80% of wild-type NCX1 (not shown). Although CuPhe was not used in this experiment, some 2-Tag-C122 becomes cross-linked without the aid of catalysis as detected with the C2C12 antibody (bottom panel of Figure 5A). Some spontaneous dimerization occurred in about 50% of experiments.

Our pull-down approach was to coexpress untagged C122 with 2-Tag-C122 or untagged cysteine-less with 2-Tag-cysteine-less in the High Five cells. We then induced cross-linking with CuPhe at 37 °C. Cells were solubilized and incubated with a Ni affinity column to pull down the 2-Tag-NCX1. Protein bound to the resin was eluted with imidazole. The eluate should contain the tagged NCX1 and, if there was interaction between exchangers, the untagged NCX1.

We tested for coprecipitation of untagged NCX1 in the pull-down fraction using immunoblots probed with R3F1. In Figure 5B, lanes 1 and 2, pull-downs of the cysteine-less proteins are shown. With this pair of proteins, only a faint band at 120 kDa was detected. The intensity of this band varied with extent of washing and may be due to nonspecific binding of untagged NCX1 to the resin or to a weak noncovalent interaction between tagged and untagged exchangers.

In lanes 3 and 4 of Figure 5B, results from pull-down experiments with coexpressed C122 and 2-Tag-C122 are shown. In this case, untagged C122 protein can be detected in a 240 kDa band only in the sample that was pretreated with CuPhe (lane 4). This experiment was repeated 9 times, and in each case, the CuPhe-treated sample displayed an intense band at 240 kDa that was absent or much reduced without CuPhe treatment. We conclude that the Ni-affinity resin pulls down a disulfide-bonded complex between tagged and untagged NCX1.

Dimer Formation with Other Single-Cysteine Mutants. Dimer formation would likely occur at a protein surface rather than at a single residue. Thus, we searched for other residues that might be involved in dimer formation. We examined other mutants with a cysteine introduced into the α-1 (C126, C127) or α-2 (C845, C854) repeat regions or in transmembrane segments (Figure 1). Residue 126 is modeled to be toward the center of the protein since residue 125 is accessible from both sides of the membrane (*17*). Mutant C126 formed dimers without the need for catalysis by CuPhe (Figure 6A). Unlike C122 (Figure 3), dimer formation was substrate independent (not shown). Because the transport activity of mutant C126 is very low (Figure 6B), we attempted to improve expression of activity. We have observed that insertion of the StrepII tag often enhanced the activity of mutants, and we generated mutant S-Tag-C126. In High Five cells, S-Tag-C126 protein still displayed low activity. Thus, we tried an alternative cell line, HEK 293 cells, for expression of this mutant. S-Tag-C126 expressed about 20% of wild-type NCX1 activity in HEK cells (Figure 6B), and only the 240 kDa band was observed on SDS−PAGE (Figure 6A). The combination of higher activity and an abundant signal at 240 kDa suggests that the active plasma membrane form of S-tag-C126 is a dimer.

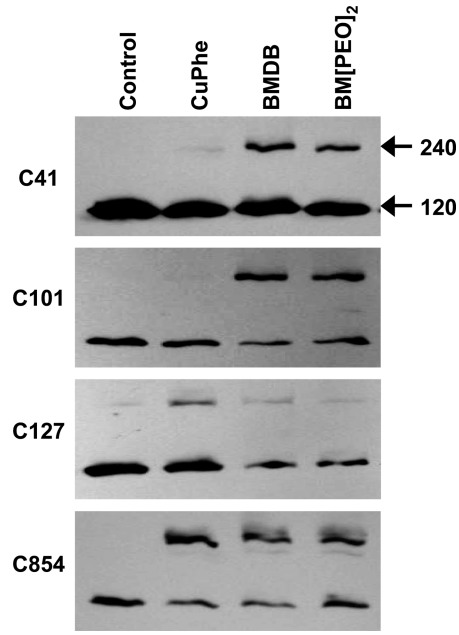

FIGURE 7: Dimerization detected in other single cysteine mutants of NCX1. High Five cells expressing the indicated mutants were treated with CuPhe or cross-linking reagents BMDB or $BM[PEO]_2$ as described in Materials and Methods before SDS−PAGE and Western blot analysis with the antibody R3F1.

To examine the functional significance of the disulfide bond between C126 exchangers, we performed Na^+-dependent $^{45}Ca^{2+}$ uptake assays in the presence and absence of the reducing reagent TCEP (5 mM) using HEK cells. Unfortunately, TCEP decreased the activity of even the cysteine-less exchanger (not shown). Thus, we were unable to determine if the intermolecular disulfide bond has any effect on activity.

We looked for cross-linking using other cysteine mutants (Figure 1). Only C127 and C854 of the two putative reentrant loops displayed CuPhe-induced cross-linking. The extent of cross-linking was low for C127. In addition, 240 kDa dimer bands were observed for mutants C41 and C101 when treated with cross-linkers BMDB or $BM[PEO]_2$ (Figure 7). These homobifunctional cross-linkers have spacer arms of 10.2 and 14.7 Å, respectively. No apparent dimer bands were observed with single-cysteine mutants C45, C49, C210, C767, C806, C845, and C877 (not shown). These mutants all had activity that was at least 10% of that of wild-type NCX1. Additional mutants with less than 10% of wild-type activity (C135, C839, C892, and C915) were not analyzed further.

DISCUSSION

Membrane proteins may exist as monomers, dimers, or higher order oligomers. For some proteins, oligomerization is essential. Many potassium channels, for example, are tetramers with each subunit forming a portion of the ion conduction pathway. For other membrane proteins, oligomerization is not necessary for activity. For example, the bumetanide-sensitive Na^+-K^+-$2Cl^-$ cotransporter forms a dimer, but each subunit transports Na^+ independently (*18*). In this study, we begin to explore the oligomeric state of the cardiac Na^+−Ca^{2+} exchanger, NCX1 by inducing covalent cross-links between NCX1 proteins and then detecting dimers on gels or after pull-down experiments. It is noteable that NCX1 dimers were only detected in pull-down experiments after inducing covalent cross-links. Thus, the interaction between pairs of NCX1 proteins must be relatively weak and can be disrupted by DDM, a gentle detergent.

In a previous study (*1*), we deduced that there was a large amount of flexibility in the vicinity of residue C768 in TMS 6 since this residue can form intramolecular cross-links with residues near either the extra- or intracellular surfaces. Here, we find that formation of the intramolecular cross-link between C122 and C768 is substrate dependent. That is, disulfide bond formation is dependent on the conformational state of the exchanger. In the course of these studies, we observed apparent dimerization of the exchanger due to cross-links between cysteines at position 122 on adjacent proteins. When both C122 and C768 were present, intramolecular cross-linking was favored in the presence of the substrate Na^+. Replacement of Na^+ with Cs^+ induced dimer formation, especially at 37 °C (Figures 2 and 3). Thus, Na^+ alters the relative distances between positions 122 and 768 on one protein and between position 122 of two adjacent proteins.

Both C122 and C768 are native cysteines that were reintroduced into the cysteine-less NCX1 background. C122 is in the α-1 repeat region composed of parts of TMS 2 and 3 connected by a reentrant loop. C122 is modeled to be at the extracellular surface of TMS 2 (Figure 1). The reentrant loop may form part of an ion conduction pathway with residue 125 being accessible to both the intracellular and extracellular medium (*17*). The TMS 3 portion of the α-1 repeat is clearly involved in ion transport as mutations of this TMS alter the apparent affinity for transported Na^+ (*19*). Detailed mutational analysis also implicates TMS 2 as being involved in ion translocation (*20, 21*). Na^+-dependent accessibility of residue 122 fits nicely into a model that defines the α-1 repeat region as being an integral part of the ion transport process.

We had previously modeled the two reentrant loops to be located within the interior of the exchanger protein (*7*) and perhaps interacting to form a portion of the ion conduction pathway. However, there was little data to support this contention. Our new results show dimer formation between cysteines in either the α-1 (C122, C126, and C127) or the α-2 repeats (C854). Thus, the α-repeats are not entirely embedded within an NCX1 protein. Instead, the α-repeats, especially the putative reentrant loops, are accessible to interact with another NCX protein.

Our data give some additional insights regarding the α-repeats. C122, near the extracellular surface of the α-1 repeat, shows a substrate-dependent change in accessibility. In contrast, however, the accessibility of C126, modeled to be deep within the reentrant loop (Figure 1), is unchanged by substrate. C126 has such a strong preference to dimerize that CuPhe catalysis is not required (Figure 6). Mutant C126 also displays low activity (Figure 6 and ref *13*.). We speculate that dimerization at C126 may hinder ion movement perhaps via inhibition of a conformational change (although the mutation itself may also decrease exchanger activity). In the α-2 repeat, C854 could also be cross-linked via reagents of varying lengths. This may indicate that the α-2 reentrant loop is flexible and spends time in different conformations.

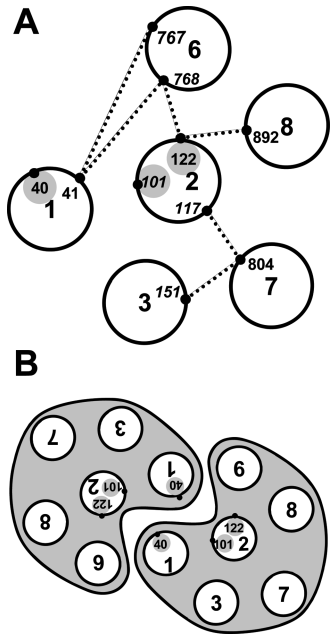

FIGURE 8: Models of NCX1 helix packing and dimerization. (A) Alternative helix packing model to allow for dimerization between NCX1 monomers at residues 40, 101, or 122. Some experimentally determined intramolecular cross-links (*1, 7*) are shown with dotted lines. Residues capable of forming intermolecular cross-links are highlighted with gray circles. TMSs 4, 5, and 9 are not included because intramolecular cross-linking data are not available, and the locations of these TMSs are not part of our helix packing model. (B) Model for dimerization between NCX1 monomers.

NCX1 dimers could also be observed when cysteines were introduced at the extracellular surface of TMS 1 (C41) or the intracellular surface of TMS 2 (C101). In these cases, cross-linking was not induced by CuPhe but required the use of cross-linking reagents that act over a larger distance. In contrast, we did not see dimer formation with cysteine mutations in TMSs 6, 7, or 8. Thus, NCX1 appears to dimerize along a specific surface of the protein rather than randomly. These data indicate the NCX1 dimerization face includes parts of TMS 1, TMS 2, and both putative reentrant loops.

We have previously presented a model for helix packing within individual NCX1 proteins based on intramolecular cross-linking studies (*1*). TMS 2 was modeled to be located toward the center of NCX1. However, with minor modifications of the model (Figure 8A), one surface of TMS 2 can face the exterior of the protein as required by our dimerization studies. Proximity of residues that can undergo intramolecular cross-linking is maintained. This results in a kidney bean shaped molecule that can interact with another NCX1 molecule at the concave surface. Since at least parts of the α-1 and α-2 repeats (residues 126, 127 and 854), which may form reentrant loops (*22, 23*), can also form dimeric interactions with another NCX1, these loops could partially line the concave surface (not shown).

Residue 122 of TMS2 interacts with residue 768 of TMS8 in the presence of the substrate Na^+. In the absence of Na^+, residue 122 becomes less accessible to residue 768 and more accessible to residue 122 in a nearby NCX1 molecule. This may occur via rotation of TMS2 and/or deocclusion of residue 122, perhaps by movement of the α-1 repeat.

It should also be noted that there is ambiguity as to the exact ends of the TMSs. Both residues 101 and 122, modeled to be at the NH_2- and CO_2H-termini of TMS2, respectively, may both extend away from TMS2 by several angstroms. Thus, the constraints placed on our helix packing model by our dimerization data are unclear.

Our data do not determine if NCX monomers act independently, like $Na^+/Ca^{2+}-K^+$ exchanger monomers, or in concert to transport ions. The apposition of portions of NCX1 that are involved in ion transport suggests possible functional consequences of dimer formation. For example, the ion transport sites from apposed exchangers may combine to form a single ion transport site or the presence of one exchanger might modulate the activity of another exchanger. If NCX1 does function as a dimer, then an added level of physiologic complexity may arise since different NCX gene isoforms (NCX1, NCX2, and NCX3) as well as different splice variants can be present in the same tissue (*24*). Although we refer to the oligomeric state of NCX1 as a dimer, higher order oligomers may form. Higher order oligomers would not be detected by the methods used in this study.

In this work, we present the first biochemical data indicating that the Na^+-Ca^{2+} exchanger, NCX1, is capable of forming dimers. We have previously presented preliminary biophysical data that are consistent with this conclusion. Fluorescence resonance energy transfer between green fluorescent protein-NCX1 fusion proteins demonstrates that NCX1 proteins are in proximity (*25*). As with other membrane proteins, we anticipate the task of determining the role of NCX dimerization in transport function to be an arduous but fruitful endeavor.

ACKNOWLEDGMENT

We thank Michela Ottolia (University of California, Los Angeles) for her assistance with densitometric analyses.

REFERENCES

1. Ren, X., Nicoll, D. A., and Philipson, K. D. (2006) Helix packing of the cardiac Na^+-Ca^{2+} exchanger: proximity of transmembrane segments 1, 2, and 6. *J. Biol. Chem. 281*, 22808–22814.
2. Hinata, M., and Kimura, J. (2004) Forefront of Na^+/Ca^{2+} exchanger studies: stoichiometry of cardiac Na^+/Ca^{2+} exchanger; 3:1 or 4:1? *J. Pharmacol. Sci. 96*, 15–18.
3. Fujioka, Y., Komeda, M., and Matsuoka, S. (2000) Stoichiometry of Na^+-Ca^{2+} exchange in inside-out patches excised from guinea-pig ventricular myocytes. *J. Physiol. 523 Pt*, 339–351.
4. Kang, T. M., Steciuk, M., and Hilgemann, D. W. (2002) Sodium-calcium exchange stoichiometry: is the noose tightening? *Ann. N.Y. Acad. Sci. 976*, 142−151; discussion 152−143.
5. Bers, D. M. (2001) Excitation-Contraction Coupling and Cardiac Contractile Force, Kluwer Academic Publishers, Norwell, MA.
6. Hilge, M., Aelen, J., and Vuister, G. W. (2006) Ca^{2+} regulation in the Na^+/Ca^{2+} exchanger involves two markedly different Ca^{2+} sensors. *Mol. Cell 22*, 15–25.
7. Qiu, Z., Nicoll, D. A., and Philipson, K. D. (2001) Helix packing of functionally important regions of the cardiac Na^+-Ca^{2+} exchanger. *J. Biol. Chem. 276*, 194–199.
8. Philipson, K. D., Longoni, S., and Ward, R. (1988) Purification of the cardiac Na^+-Ca^{2+} exchange protein. *Biochim. Biophys. Acta 945*, 298–306.
9. Santacruz-Toloza, L., Ottolia, M., Nicoll, D. A., and Philipson, K. D. (2000) Functional analysis of a disulfide bond in the cardiac Na^+-Ca^{2+} exchanger. *J. Biol. Chem. 275*, 182–188.
10. Cai, X., and Lytton, J. (2004) The cation/Ca^{2+} exchanger superfamily: phylogenetic analysis and structural implications. *Mol. Biol. Evol. 21*, 1692–1703.
11. Bauer, P. J., and Drechsler, M. (1992) Association of cyclic GMP-gated channels and Na^+-Ca^{2+}-K^+ exchangers in bovine retinal rod outer segment plasma membranes. *J. Physiol. 451*, 109–131.

12. Schwarzer, A., Kim, T. S., Hagen, V., Molday, R. S., and Bauer, P. J. (1997) The Na/Ca-K exchanger of rod photoreceptor exists as dimer in the plasma membrane. *Biochemistry 36*, 13667–13676.
13. Kang, K., Bauer, P. J., Kinjo, T. G., Szerencsei, R. T., Bonigk, W., Winkfein, R. J., and Schnetkamp, P. P. (2003) Assembly of retinal rod or cone Na^+/Ca^{2+}-K^+ exchanger oligomers with cGMP-gated channel subunits as probed with heterologously expressed cDNAs. *Biochemistry 42*, 4593–4600.
14. Porzig, H., Li, Z., Nicoll, D. A., and Philipson, K. D. (1993) Mapping of the cardiac sodium-calcium exchanger with monoclonal antibodies. *Am. J. Physiol. 265*, C748–756.
15. Abramoff, M. D., Magelhaes, P. J., and Ram, S. J. (2004) Image processing with ImageJ. *Biophotonics Int. 11*, 36–42.
16. Nicoll, D. A., Ottolia, M., Lu, L., Lu, Y., and Philipson, K. D. (1999) A new topological model of the cardiac sarcolemmal Na^+-Ca^{2+} exchanger. *J. Biol. Chem. 274*, 910–917.
17. Iwamoto, T., Uehara, A., Imanaga, I., and Shigekawa, M. (2000) The Na^+/Ca^{2+} exchanger NCX1 has oppositely oriented reentrant loop domains that contain conserved aspartic acids whose mutation alters its apparent Ca^{2+} affinity. *J. Biol. Chem. 275*, 38571–38580.
18. Starremans, P. G., Kersten, F. F., Van Den Heuvel, L. P., Knoers, N. V., and Bindels, R. J. (2003) Dimeric architecture of the human bumetanide-sensitive Na-K-Cl Co-transporter. *J. Am. Soc. Nephrol. 14*, 3039–3046.
19. Ottolia, M., Nicoll, D. A., and Philipson, K. D. (2005) Mutational analysis of the alpha-1 repeat of the cardiac Na^+-Ca^{2+} exchanger. *J. Biol. Chem. 280*, 1061–1069.
20. Doering, A. E., Nicoll, D. A., Lu, Y., Lu, L., Weiss, J. N., and Philipson, K. D. (1998) Topology of a functionally important region of the cardiac Na^+/Ca^{2+} exchanger. *J. Biol. Chem. 273*, 778–783.
21. Nicoll, D. A., Hryshko, L. V., Matsuoka, S., Frank, J. S., and Philipson, K. D. (1996) Mutagenesis studies of the cardiac Na^+-Ca^{2+} exchanger. *Ann. N.Y. Acad. Sci. 779*, 86–92.
22. Iwamoto, T., Nakamura, T. Y., Pan, Y., Uehara, A., Imanaga, I., and Shigekawa, M. (1999) Unique topology of the internal repeats in the cardiac Na^+/Ca^{2+} exchanger. *FEBS Lett. 446*, 264–268.
23. Nicoll, D. A., Hryshko, L. V., Matsuoka, S., Frank, J. S., and Philipson, K. D. (1996) Mutation of amino acid residues in the putative transmembrane segments of the cardiac sarcolemmal Na^+-Ca^{2+} exchanger. *J. Biol. Chem. 271*, 13385–13391.
24. Quednau, B. D., Nicoll, D. A., and Philipson, K. D. (1997) Tissue specificity and alternative splicing of the Na^+/Ca^{2+} exchanger isoforms NCX1, NCX2, and NCX3 in rat. *Am. J. Physiol. 272*, C1250–1261.
25. Ottolia, M., John, S., Xie, Y., Ren, X., and Philipson, K. D. (2007) Shedding light on the Na^+/Ca^{2+} exchanger. *Ann. N.Y. Acad. Sci. 1099*, 78–85.

BI800177T